The Scent of Maibowle – π Electron Localization in Coumarin from Its Microwave-Determined Structure

Ha Vinh Lam Nguyen, Jens-Uwe Grabow

▶ **To cite this version:**

Ha Vinh Lam Nguyen, Jens-Uwe Grabow. The Scent of Maibowle – π Electron Localization in Coumarin from Its Microwave-Determined Structure. ChemPhysChem, 2020, 21 (12), pp.1243-1248. 10.1002/cphc.202000234 . hal-03182668

HAL Id: hal-03182668
https://hal.u-pec.fr/hal-03182668v1

Submitted on 26 Mar 2021

HAL is a multi-disciplinary open access archive for the deposit and dissemination of scientific research documents, whether they are published or not. The documents may come from teaching and research institutions in France or abroad, or from public or private research centers.

L'archive ouverte pluridisciplinaire **HAL**, est destinée au dépôt et à la diffusion de documents scientifiques de niveau recherche, publiés ou non, émanant des établissements d'enseignement et de recherche français ou étrangers, des laboratoires publics ou privés.

The scent of maibowle – π electron localization in coumarin from its microwave-determined structure

Ha Vinh Lam Nguyen*[a] and Jens-Uwe Grabow[b]

This work is dedicated to T. Bell.

Abstract: The microwave spectra of the natural substance coumarin, a planar aromatic molecule with the specific scent of maibowle, a popular fruit punch served in spring and early summer, were recorded using a molecular jet Fourier transform microwave spectrometer working in the frequency range from 4.0 to 26.5 GHz. The rotational constants and centrifugal distortion constants were determined with high precision, reproducing the spectra to experimental accuracy. The spectra of all singly-substituted ^{13}C and ^{18}O isotopologues were observed in their natural abundances to determine the experimental heavy atom substitution r_s and semi-experimental equilibrium r_e^{SE} structures. The experimental bond lengths and bond angles were compared to those obtained from quantum chemical calculations and those of related molecules reported in the literature with benzene as the prototype. The alternation of the C-C bond lengths to the value of 1.39 Å found for benzene reflects the localization of π electrons in coumarin, where the benzene ring and the lactone-like chain −CH=CH−(C=O)−O− are fused. The large, negative inertial defect of coumarin is consistent with out-of-plane vibrations of the fused rings.

1. Introduction

Coumarin is an aromatic molecule with the structural formula $C_9H_6O_2$. With its specific, pleasant odor and its bitter taste, coumarin is a natural substance present in many plants, e.g. in vernal grasses, yellow melilot, woodruff, date, and vietnamese cinnamon [1]. It is particularly used as fragrance in the perfumery as well as in cuisine, most notably to give maibowle its very specific woodruff aroma [2].

Coumarin is produced synthetically *i.e.* in a condensation reaction between acetic anhydride and salicylaldehyde using Perkin's synthesis. From nature, the starting material for coumarin in plants is cinnamic acid, and coumarin is formed by hydroxylation, glycosidation, and cyclization. Itself being of moderate size, coumarin is a common structural part of larger biological molecules. Many molecules which have important roles in medicine, rodenticide precursors, laser dyes, perfumes, and aromatizes contain coumarin as a substructure, such as the prescriotion drug warfarin which is an anticoagulant used to inhibit formation of deep vein thrombosis, blood clots, and pulmonary embolism. 4-hydroxycoumarins are a type of vitamin K antagonist, which block the regeneration and recycling of this vitamin.

The structure of benzene, well-established by X-ray diffraction, possesses a constant C–C–C angle of 120° and a constant C–C distance of 1.39 Å between six carbon atoms, which is shorter than a C–C single bond of about 1.47 Å but greater than a C–C double bond of 1.35 Å. This is a measure for the perfect π-electron delocalization in benzene. It is known that substitutions on the benzene ring can alter structural parameters such as bond lengths and bond angles at the substituted positions. As a consequence, they break the perfect π-electron delocalization, making some regions of the aromatic system richer on π-electrons than the others. The use of pulsed molecular jet Fourier Transform microwave spectrometers has led to significant improvements in sensitivity and accuracy compared to absorption cells, enabling us to measure and study the isotopic species of all singly-substituted ^{13}C- and ^{18}O-isotopologues of coumarin. Subsequently, bond lengths and bond angles can be precisely determined to deduce information about the π-electron location in coumarin.

2. Quantum Chemical Calculations

Constrained by the rigidity of the aromatic ring, coumarin can only possess one possible, planar structure as indicated in Figure 1. Previous microwave spectroscopic studies on similar systems reported in the literature, such as those on the polycyclic aromatic hydrocarbons (PAHs) azulene, acenaphthene, acenaphthylene, and fluorene [3], polycyclic aromatic nitrogen heterocycles (PANHs) phenanthridine, acridine, and 1,10-phenanthroline [4], as well as a series of alkylnaphthalenes [5] consistently suggested that the structures of such molecules can be calculated well with the B3LYP method. The basis set was chosen to be either Dunning's cc-pVTZ [6] or Pople's 6-311+G(d,p) and 6-311++G(d,p) [7]. From our own experiences [8-11] and studies in the literature [12-15], the MP2/6-311G++(d,p) level of theory has proven its reliability in calculating rotational constants of aromatic-ring containing molecules for assignment purposes. Therefore, quantum chemical calculations at this level were carried out with the *Gaussian 16* program [16] and the *ab initio* rotational constants A = 2819.5 MHz, B = 880.0 MHz, C = 670.7 MHz were used as starting values to predict the microwave spectrum of coumarin. For comparison, the obtained structure was re-optimized at the CAM-B3LYP-D3BJ/cc-pVTZ level of theory using Grimme's dispersion correction [17], Becke-Johnson damping [18], as well as the electron mass corrections which are important in determining the equilibrium geometry of planar, aromatic molecules. We also performed calculations at the MP2/6-31G(d,p) level, since it has yielded rotational constants with

[a] Dr. Ha Vinh Lam Nguyen
Laboratoire Interuniversitaire des Systèmes Atmosphériques (LISA), CNRS UMR 7583, Université Paris-Est Créteil, Université de Paris, Institut Pierre Simon Laplace, 61 avenue du Général de Gaulle, F-94010 Créteil cedex, France. * E-mail: lam.nguyen@lisa.u-pec.fr
[b] Prof. Dr. Jens-Uwe Grabow
Institut für Physikalische Chemie und Elektrochemie, Lehrgebiet A, Callinstrasse 3a, D-30167 Hannover, Germany

Supporting information for this article is given via a link at the end of the document.

values remarkably close to those of the experimental ones for the related molecules quinoline and isoquinoline [19], as well as for some other molecules containing an aromatic ring [20-22]. The Cartesian coordinates of the optimized structure are available in Table S-1 in the Supporting Information. Anharmonic frequency calculations were performed to obtain vibrational ground state rotational constants and centrifugal distortion constants.

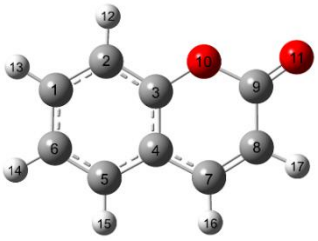

Figure 1. Structure of coumarin optimized at the MP2/6-311++G(d,p) level of theory (see text).

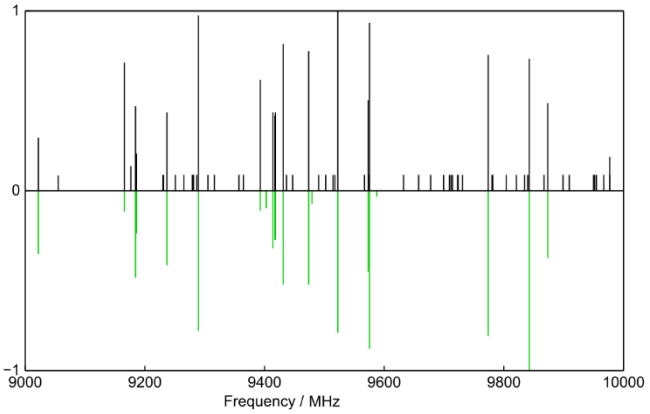

Figure 2. A portion of the broadband scan of coumarin. The frequencies are given in MHz; the intensity in arbitrary unit. The upper trace shows the experimental spectrum with all intense lines belonging to the parent species. For the weaker transitions arising from the nine ^{13}C isotopologues, only the line positions are indicated as satellite bands in black with constant intensity. The calculated spectrum of the main isotopologue is given in maibowle green on the lower trace.

3. Microwave Spectrum

3.1. Spectral assignment

At the beginning of the experiment, a broadband scan in the frequency range from 8 to 11 GHz was carried out, where about 20 intense lines and many much weaker lines are observed. A portion of the survey spectrum is shown in Figure 2. The dipole moment components calculated with the MP2 method are μ_a = 4.88, μ_b = 3.14, and μ_c = 0.0 D. Therefore, strong *a*- and *b*-type, but not *c*-type transitions were expected in the rotational spectrum. We started our assignment with *a*-type $J'' = 5 \leftarrow J' = 4$ transitions, because - from our experiences - the frequencies predicted for *a*-type lines are often quite reliable. The assignment was straightforward. Afterwards, *b*-type lines were also assigned and all 20 strong lines found in the scan could be fitted with the program *XIAM* [23] using a semi-rigid rotor model where the Hamiltonian only consists of rotational and quartic centrifugal distortion terms of Watson's S reduced Hamiltonian.

With the prediction refined from this fit, further transitions out of the scan region could be identified and measured directly. A typical spectrum is presented in Figure 3. The final fit, given as ^{12}C in Table 1, contains 162 lines with $J \leq 12$ and $K_a \leq 7$ and shows an excellent standard deviation of 1.3 kHz. A list of all measured lines can be found in Table S-2 in the Supporting Information.

After the main isotopic species was assigned, many weak lines remained in the spectrum. We assumed that they belong to the spectra of the nine ^{13}C isotopologues of coumarin. The Cartesian coordinates of the optimized structure in Figure 1 were taken, and the mass of the individual carbon atoms was adjusted to calculate the rotational constants of all ^{13}C isotopologues. The predicted ^{13}C-frequencies were correctedwith the differences between the frequencies predicted with the B_e constants obtained at the MP2/6-311++G(d,p) level and the experimental frequencies of the parent species, leading to straightforward assignments of all ^{13}C isotopologues. Transitions with $J \leq 7$ and $K_a \leq 3$ were measured. Due to the

Table 1. Spectroscopic parameters of the parent species, nine ^{13}C-isotopologues, and two ^{18}O-isotopologues of coumarin (for atom numbering, see Figure 1).

Par.[a]	Unit	^{12}C	^{13}C(1)	^{13}C(2)	^{13}C(3)	^{13}C(4)	^{13}C(5)	Calc.[b]
A	MHz	2830.370692(65)	2813.97656(22)	2796.09675(75)	2825.65025(21)	2819.79587(39)	2805.77814(90)	2811.528
B	MHz	885.581280(30)	875.01639(12)	882.926957(42)	885.492575(96)	885.157599(76)	880.200278(50)	875.068
C	MHz	674.795663(28)	667.72513(12)	671.296091(25)	674.475742(96)	673.947569(48)	670.272915(30)	667.675
D_J	kHz	0.00893(13)						0.00826
D_{JK}	kHz	0.02296(53)	0.0173(56)	0.0174(45)	0.0174(51)	0.0249(98)	0.0140(54)	0.02141
D_K	kHz	0.1687(24)						0.1627
d_1	kHz	−0.002443(73)	−0.00242(74)		−0.00407(68)			−0.002374
d_2	kHz	−0.000432(30)						−0.000406
σ[c]	kHz	1.3	0.7	0.6	0.7	1.2	0.7	
N[d]		162	14	13	14	14	13	
		^{13}C(6)	**^{13}C(7)**	**^{13}C(8)**	**^{13}C(9)**	**^{18}O(10)**	**^{18}O(11)**	
A	MHz	2828.61467(58)	2784.61352(67)	2807.11546(18)	2829.70926(24)	2796.76921(22)	2814.8637(80)	
B	MHz	872.67458(27)	885.03645(51)	880.276698(93)	878.78450(13)	882.555582(10)	855.26121(51)	
C	MHz	667.17917(32)	671.84377(55)	670.394192(94)	670.80478(13)	671.123344(7)	656.18790(24)	
D_J	kHz	0.0117(33)	0.0146(43)					
D_{JK}	kHz			0.0243(45)	0.0139(63)			
d_1	kHz		-0.0126(24)	-0.00230(60)	-0.00285(83)			
σ[c]	kHz	1.8	2.2	0.6	0.8	0.1	3.5	
N[d]		14	12	14	13	6	7	

[a] All parameters refer to the principal axis system. Watson's S reduction in I^r representation was used. Standard errors in parentheses are in the unit of the least significant digits. For all ^{13}C and ^{18}O-isotopologues, the values of centrifugal distortion constants which are not fitted are fixed to those of the parent species. [b] Ground state rotational constants and centrifugal distortion constants from anharmonic frequency calculations at the MP2/6-31G(d,p) level of theory. [c] Standard deviation of the fit. [d] Number of lines.

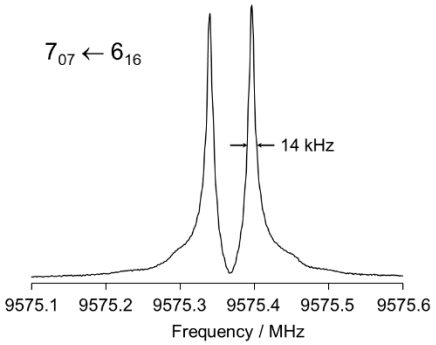

Figure 3. A typical $J''_{K''_a K''_c} \leftarrow J'_{K'_a K'_c}$ rotational transition of coumarin. The line width is 14 kHz (full width at half height). The doublet arises from the Doppler effect; the mean frequency is 9575.3680 MHz. For this spectrum, 1000 free-induction decays were co-added and averaged.

small number of observable lines, only one or two quartic centrifugal distortion constants could be determined while the values of the other distortion constants were fixed to those of the parent species. The spectroscopic parameters of the ^{13}C isotopologues are summarized in Table 1 along with those of the parent species; the frequency lists are given in Table S-3 in the Supporting Information.

To complete the heavy atom structure, we also searched for the two ^{18}O-isotopologues. Because of the low natural abundances of 0.2%, transitions of these species were not visible in the broadband scan given in Figure 2 where only 200 co-added decays were taken per each scan step of 0.25 MHz. Therefore, scans of ±2 MHz around the corrected frequencies of three *a*-type transitions $6_{06} \leftarrow 5_{05}$, $6_{15} \leftarrow 5_{14}$, and $7_{07} \leftarrow 6_{06}$ were performed by steps of 0.2 MHz with 10000 co-added decays at each step. In total, 6 lines could be found for the ^{18}O(10) and 7 lines for the ^{18}O(11) species. In the fits, all quartic centrifugal distortion constants were fixed to the values of the parent species.

3.2. Structure determinations

The rotational constants of the parent species as well as those of the ^{13}C and ^{18}O-isotopologues given in Table 1 were input in the programs KRA and EVAL available at the PROSPE website [24] to determine the heavy atom substitution r_s structure of coumarin using Kraitchman's equations [25]. Since the atom coordinates appear squared in these equations, their signs are ambiguous and were taken from the optimized geometry. Costain's rule was used to determine the uncertainties [26]. The atom coordinates output by the program KRA are given in Table 2; the bond lengths and bond angles obtained from the program EVAL are presented in Table 3 and Figure 4. For the EVAL input, all values of the *c*-coordinates were set to zero.

Though the substitution r_s structure is quite often reported in the literature, it is known that this structure determination is not reliable for large molecules such as coumarin exhibiting one or more atoms near one of the principal axes and Costain's rule is over-optimistic [27]. For this reason, the semi-experimental equilibrium r_e^{SE} structure might be a better alternative. The

Table 2. Experimental atom positions from the substitution r_s and semi-experimental equilibrium r_e^{SE} structures of coumarin. Due to planarity, all *c*-coordinates were set to zero. The equilibrium atom positions r_e are optimized at the MP2/6-31G(d,p) level of theory. Standard errors in parentheses are in the unit of the least significant digits.

	r_s		$r_{s\rightarrow e}^{SE}$	
	a/Å	*b*/Å	*a*/Å	*b*/Å
C(1)	2.62603(57)	–1.0306(15)	2.62084(57)	–1.0299(15)
C(2)	1.3084(12)	–1.4853(11)	1.3114(12)	–1.4832(11)
C(3)	0.2392(63)	–0.5471(28)	0.2690(56)	–0.5512(28)
C(4)	0.5230(29)	0.8199(19)	0.5292(29)	0.8211(19)
C(5)	1.86732(80)	1.2587(12)	1.86656(80)	1.2578(12)
C(6)	2.90977(52)	0.3362(45)	2.90311(52)	0.3402(45)
C(7)	–0.5937(26)	1.71746(88)	–0.6009(26)	1.71428(88)
C(8)	–1.85403(81)	1.2235(12)	–1.84860(81)	1.2224(12)
C(9)	–2.10449(71)	–0.2061(73)	–2.10317(71)	–0.2182(69)
O(10)	–0.99158(16)	–1.0438(15)	–0.9969(16)	–1.0411(15)
O(11)	–3.19574(47)	–0.7276(21)	–3.19019(47)	–0.7247(21)
	r_e		$r_{0\rightarrow e}^{SE}$	
C(1)	2.63179	–1.03739	–2.6210(47)	–1.030(13)
C(2)	1.31644	–1.48807	–1.3119(96)	–1.4834(87)
C(3)	0.28051	–0.55162	–0.276(13)	–0.551(22)
C(4)	0.54065	0.82802	–0.532(18)	0.821(16)
C(5)	1.87911	1.26021	–1.8668(67)	1.258(11)
C(6)	2.91574	0.33681	–2.9032(43)	0.342(20)
C(7)	–0.59127	1.71955	0.597(19)	1.7149(75)
C(8)	–1.85094	1.22513	1.8483(65)	1.223(11)
C(9)	–2.11872	–0.21095	2.1029(64)	–0.223(23)
O(10)	–1.00008	–1.04683	0.9965(65)	–1.0416(66)
O(11)	–3.21970	–0.72626	3.1898(22)	–0.7236(94)
H(12)	1.06981	–2.54115	–1.069(30)	–2.531(68)
H(13)	3.44088	–1.75623	–3.427(56)	–1.743(44)
H(14)	3.94306	0.67613	–3.923(69)	0.683(30)
H(15)	2.08683	2.32383	–2.068(22)	2.315(68)
H(16)	–0.41946	2.78996	0.424(43)	2.777(68)
H(17)	–2.72393	1.86131	2.718(58)	1.856(40)

Table 3. Bond lengths (in Å) and bond angles (in degrees) of coumarin deduced from the substitution r_s, semi-experimental equilibrium r_e^{SE}, and r_e equilibrium structures. Standard errors in parentheses are in the unit of the least significant digits.

	r_s	$r_{s\rightarrow e}^{SE}$	$r_{0\rightarrow e}^{SE}$[a]	r_e[b]
C1–C2	1.3938(14)	1.3857(14)	1.385(14)	1.3904
C2–C3	1.4225(52)	1.3983(47)	1.394(20)	1.3965
C3–C4	1.3961(36)	1.3967(35)	1.395(29)	1.4040
C4–C5	1.4142(30)	1.4069(29)	1.404(18)	1.4065
C5–C6	1.3920(32)	1.3844(32)	1.383(18)	1.3883
C1–C6	1.3960(47)	1.3989(46)		1.4032
C4–C7	1.4327(33)	1.4405(33)	1.441(28)	1.4409
C7–C8	1.3537(26)	1.3412(26)	1.344(22)	1.3532
C8–C9	1.4513(73)	1.4629(69)	1.469(28)	1.4608
C9–O10	1.3930(47)	1.3788(45)	1.375(18)	1.3964
C3–O10	1.3273(61)	1.3574(55)		1.3730
C9–O11	1.2095(34)	1.1992(32)	1.196(12)	1.2156
C1–C2–C3	119.70(21)	119.10(20)	118.9(886)	118.97
C2–C3–C4	119.54(44)	121.07(41)		121.43
C3–C4–C5	119.80(31)	118.82(30)	118.7(13)	118.57
C4–C5–C6	120.42(18)	120.40(18)	120.4(11)	120.41
C5–C6–C1	119.78(12)	119.88(12)		120.02
C6–C1–C2	120.764(97)	120.737(97)		120.59
C3–C4–C7	117.06(32)	117.59(31)	117.8(13)	117.55
C4–C7–C8	119.81(13)	120.16(13)	120.2(11)	120.34
C7–C8–C9	121.34(11)	121.54(11)	121.44(621)	121.99
C8–C9–O10	117.03(21)	116.62(20)	116.50(74)	116.21
C3–O10–C9	121.05(31)	122.20(29)		122.09
C4–C3–O10	123.71(40)	121.89(36)		121.82
C8–C9–O11	125.48(38)	125.00(36)	124.7(16)	125.64

[a] All hydrogen atom's bond lengths were fitted to be 1.076(74) Å but constrained to be the same. [b] Geometry optimized at the MP2/6-31G(d,p) level of theory.

determination is shown *i.a.* in Refs. [20,27-32]. For a comparison with the r_s structure, we first determined the so-called $r_{s\rightarrow e}^{SE}$ structure, where the experimental ground state rotational constants A_0, B_0, and C_0 of the parent species and all isotopologues given in Table 1 are rovibrationally corrected from the *ab initio* cubic force field at the MP2/6-31G(d,p) level of

theory before inputting them in the program KRA [24] (for details, see Table S-4 in the Supporting Information). Nevertheless, $r_{s\rightarrow e}^{SE}$ is a partial structure determination since only spectra of heavy atoms could be measured and the locations of hydrogen atoms remained unknown. However, hydrogen coordinates predicted by quantum chemistry can be fitted together with the corrected A_0, B_0, and C_0 rotational constants using the program STRFIT [33], yielding the $r_{0\rightarrow e}^{SE}$ structure. In the fit, the hydrogen atom locations were varied, but all C–H bond lengths are constrained to be the same. The atom coordinates, bond lengths, and bond angles of both r_e^{SE} structures are also given in Tables 2 and 3.

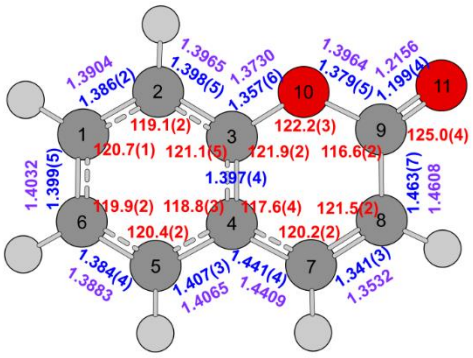

Figure 4. Experimental bond lengths (blue, in Å) and bond angles (red, in degrees) of coumarin from the semi-experimental equilibrium $r_{s\rightarrow e}^{SE}$ structure. Bond lengths from the equilibrium r_e structure calculated at the MP2/6-31G(d,p) level of theory (purple, in Å) are also given for comparison. Standard errors in parentheses are in the unit of the least significant digit.

4. Discussion

4.1. Molecular geometry

The well-established structure of benzene determined by X-ray diffraction shows the same bond length of 1.39 Å between six carbon atoms, which is shorter than a C–C single bond of about 1.47 Å but greater than a C–C double bond of 1.35 Å. This constant, intermediate C–C distance in benzene implies a perfect electron delocalization where the π electrons are distributed equally within the ring. Examinations of other aromatic compounds related to benzene, e.g. naphthalene, anthracene, and phenanthrene, disclose that for example in naphthalene, four bonds are shorter (1.37 Å) and have about two times greater double bond character than the other six bonds (1.42 Å) [34]. Obviously, the π electron delocalization is perturbed by the less symmetric structure compared to that of benzene. In coumarin, the perturbations of bond lengths in benzene are even more pronounced due to the insertion of the lactone moiety into the ring fused with benzene, which breaks the perfect delocalization of benzene due to angle strains (known as the Mills-Nixon effect [35]). While the distance between the carbon atom in the benzene part of coumarin are essentially equal to the value of 1.39 Å reported for solid benzene (see Figure 4 for atom numbering and values), the π electron delocalization is significantly perturbed in the other half part containing the lactone group, and is clearly reflected in the bond lengths. The distance of 1.341(3) Å between C(7) and C(8) as well as 1.357(6) Å between C(3) and O(10) implies that both C7–C8 and C9–O10 have a great double bond character. The C9–O10 bond length of 1.379(5) Å is similar to the values of the C–C bond lengths in the benzene part. However, it is greater than the value of 1.35 Å found for the (O=)C–O bond of *s-cis*-methacrylic acid (MAA) and *s-cis*-methyl methacrylate (MMA) [32], marked in blue in Figure 5. The C8–C9 bond length of 1.4678 Å reflects slightly less single bond character than the comparable (O=)C–C bond of MAA and MMA (1.48 Å), shown in red in Figure 5. These differences can be also explained by angle strains at the oxygen atom arising from ring fusion, which does not affect much the length of the C7–C8 bond (marked in green in Figure 5, 1.34 Å in coumarin, MAA, and MMA). Finally, the C9–O10 bond is also not perturbed and has the same length as that found for MAA and MMA, as well as that of 2-thiophenecarboxaldehyde (2TPC) [28] (1.20 Å in all cases). We note that all values of MAA, MMA, and 2TPC also refer to the r_e^{SE} structure, and thus ensure a reasonable comparison without influence of vibrations.

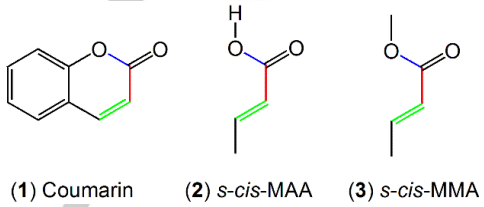

Figure 5. Comparison of some bond lengths of coumarin (**1**) with those of the open chain molecules *s-cis*-methacrylic acid (2) and *s-cis*-methyl methacrylate (**3**) (see text).

4.2. Inertial defect

With all atoms located on the *ab*-plane, we expected an inertial defect very close to zero, as observed for *e.g.* pyrrole (0.017 uÅ^2) [36], oxazole (0.056 uÅ^2) [37], 2TPC (0.008 uÅ^2) [28], and fluorobenzene (0.033 uÅ^2), but surprisingly found $\Delta_c = I_c - I_a - I_b$ = –0.294 uÅ^2. Such negative, large values have been observed for many molecules related to coumarin such as the PAHs [3] and PANHs [4] mentioned in Section 2, as well as 9-cyanoanthracene [38], quinolone [19], and isoquinoline [19], which could be traced back to significant out-of-plane vibrations of the rings [39]. The small, positive inertial defect is well-known as a judgement for the planarity of small molecules. The abnormally large, negative inertial defect due to out-of-plane ring motions has been found in a considerable number of molecules containing aromatic rings [40].

4.3. Theory versus experiment

The equilibrium rotational constants B_e calculated at the MP2/6-31G(d,p) level of theory are in remarkable agreement with the experimental results, as shown in Table 4. Though comparing predicted B_e constants with experimental B_0 constants is not physically meaningful, it shows that the MP2/6-31G(d,p) level offers cost-efficient calculations with sufficient accuracy for spectral assignment purposes. The MP2/6-311++G(d,p) is a higher level than MP2/6-31G(d,p) and therefore, purely from theoretical perspective, more accurate. However, the errors of the MP2/6-31G(d,p) level compensate with the missing $B_e - B_0$ corrections in a way, that the B_e calculated rotational constants accidentally match the B_0 experimental constants. Therefore, this level is useful for assigning microwave spectra of aromatic molecules like coumarin.

Table 4. Equilibrium rotational constants A_e, B_e, C_e (in MHz), vibrational ground state rotational constants A_0, B_0, C_0 (in MHz) of coumarin calculated at different levels of theory.

	MP2 /6-311++G(d,p)	MP2 /6-31G(d,p)	B3LYP-D3BJ /cc-pVTZ	Exp.
A	2819.5	2829.2	2874.5	2830.4
B	880.0	879.6	894.8	885.6
C	670.7	671.0	682.4	674.8

5. Conclusions

The interplay between high-resolution pulsed jet microwave spectroscopy and quantum chemistry yields accurate molecular parameters of coumarin in the gas phase. The spectra of all singly-substituted heavy atom isotopologues were assigned, enabling the determination of the substitution r_s and semi-experimental equilibrium r_e^{SE} structures. The resulting bond lengths and bond angles were used to evaluate the perturbation in the π electron delocalization within the aromatic ring. The large and negative value found for the inertial defect of coumarin could be explained by out-of-plane motions of the ring, as observed for other related molecules. Comparison of the experimental and calculated rotational constants has shown that error compensations at the MP2/6-31G(d,p) level result in accidentally good values for spectral assignment purposes.

Experimental Section

The rotational spectra were measured with a coaxially oriented beam-resonator arrangement (COBRA) spectrometer operating in the frequency range from 4 to 26.5 GHz. Details of the spectrometer were described elsewhere [41] already. Coumarin was purchased from Merck Schuhard, Hohenbrunn, Germany, with a stated purity of over 98 % and used without further purification. For the measurements, the solid substance coumarin was placed onto some glass wool which was put near the expansion nozzle inside the soleniod valve and heated to 75°C. Helium at a pressure of approximately 200 kPa flows over the sample slowly to saturate. The helium-coumarin mixture was expanded through the pulsed nozzle into the cavity.

Acknowledgements

This work was supported by the Agence Nationale de la Recherche ANR (project ID ANR-18-CE29-0011). J.-U.G. thanks the Deutsche Forschungsgemeinschaft (DFG) and the Land Niedersachsen for funds.

Keywords: microwave spectroscopy • rotational spectroscopy • coumarin • isotopologue • structural determination

[1] Y.-H. Wang, B. Avula, N. P. D. Nanayakkara, J. Zhao, I. A. Khan, *J. Agric. Food Chem.* **2013**, *61*, 4470–4476.

[2] J. Daphi-Weber, H. Raddatz, R. Müller, Untersuchung von Riechstoffen – Kontrollierte Düfte, *Gesellschaft Deutscher Chemiker*, **2010**, ISBN 978-3-936028-64-5.

[3] S. Thorwirth, P. Theulé, C. A. Gottlieb, M. C. McCarthy, P. Thaddeus, *Astrophys. J.* **2007**, *662*, 1309–1314.

[4] D. McNaughton, P. D. Godfrey, R. D. Brown, S. Thorwirth, J.-U. Grabow, *Astrophys. J.* **2008**, *678*, 309–315.

[5] E. G. Schnitzler, B. L. M. Zenchyzen, W. Jäger, *Astrophys. J.* **2015**, *805*, 141.

[6] T. H. Dunning Jr., *J. Chem. Phys.* **1989**, 90, 1007.

[7] R. Ditchfield, W. J. Hehre, J. A. Pople, *J. Chem. Phys.* **1971**, 54, 724–728.

[8] R. Hakiri, N. Derbel, H. V. L. Nguyen, H. Mouhib, *Phys. Chem. Chem. Phys.* **2018**, *20*, 25577–25582.

[9] V. Van, W. Stahl, H. V. L. Nguyen, *ChemPhysChem* **2016**, *17*, 3223–3228.

[10] V. Van, J. Bruckhuisen, W. Stahl, V. Ilyushin, H. V. L. Nguyen, *J. Mol. Spectrosc.* **2018**, *343*, 121–125.

[11] L. Ferres, H. Mouhib, W. Stahl, M. Schwell, H. V. L. Nguyen, *J. Mol. Spectrosc.* **2017**, *337*, 59–64.

[12] J. C. López , V. Cortijo , S. Blanco, J. L. Alonso, *Phys. Chem. Chem. Phys.* **2007**, *9*, 4521–4527.

[13] A. R. Conrad, N. Z. Barefoot, M. J. Tubergen, *Phys. Chem. Chem. Phys.* **2010**, 12, 8350–8356.

[14] C. Calabrese, A. Maris, L. Evangelisti, W. Caminati, S. Melandri, *ChemPhysChem* **2013**, *14*, 1943–1950.

[15] Y. Jin, T. Lu, Q. Gou, G. Feng, *J. Mol. Struct.* **2020**, *1205*, 127632.

[16] M. J. Frisch, G. W. Trucks, H. B. Schlegel, G. E. Scuseria, M. A. Robb, J. R. Cheeseman, G. Scalmani, V. Barone, G. A. Petersson, H. Nakatsuji, X. Li, M. Caricato, A. V. Marenich, J. Bloino, B. G. Janesko, R. Gomperts, B. Mennucci, H. P. Hratchian, J. V. Ortiz, A. F. Izmaylov, J. L. Sonnenberg, D. Williams-Young, F. Ding, F. Lipparini, F. Egidi, J. Goings, B. Peng, A. Petrone, T. Henderson, D. Ranasinghe, V. G. Zakrzewski, J. Gao, N. Rega, G. Zheng, W. Liang, M. Hada, M. Ehara, K. Toyota, R. Fukuda, J. Hasegawa, M. Ishida, T. Nakajima, Y. Honda, O. Kitao, H. Nakai, T. Vreven, K. Throssell, J.A. Montgomery, Jr., J. E. Peralta, F. Ogliaro, M. J. Bearpark, J. J. Heyd, E. N. Brothers, K. N. Kudin, V. N. Staroverov, T. A. Keith, R. Kobayashi, J. Normand, K. Raghavachari, A. P. Rendell, J. C. Burant, S. S. Iyengar, J. Tomasi, M. Cossi, J. M. Millam, M. Klene, C. Adamo, R. Cammi, J. W. Ochterski, R. L. Martin, K. Morokuma, O. Farkas, J. B. Foresman, D. J. Fox, Gaussian 16, Revision B.01, Inc., Wallingford CT, 2016.

[17] S. Grimme, J. Antony, S. Ehrlich, H. Krieg, *J. Chem. Phys.* **2010**, *132*, 154104.

[18] S. Grimme, S. Ehrlich, L. Goerig, *J. Comp. Chem.* **2011**, *32*, 1456–1465.

[19] Z. Kisiel, O. Desyatnyk, L. Pszczółkowski, S. B. Charnley, P. Ehrenfreund, *J. Mol. Spectrosc.* 2003, *217*, 115–122.

[20] H. V. L. Nguyen, *J. Mol. Struct.* **2020**, *1208*, 127909.

[21] L. Ferres, W. Stahl, H. V. L. Nguyen, *Mol. Phys.* **2016**, *114*, 2788–2793.

[22] L. Ferres, H. Mouhib, W. Stahl, H. V. L. Nguyen, *ChemPhysChem* **2017**, *18*, 1855–1859.

[23] H. Hartwig, H. Dreizler, *Z. Naturforsch.* **1996**, *51a*, 923–932.

[24] Z. Kisiel, PROSPE-Programs for ROtational SPEctroscopy. <http://info.ifpan.edu.pl/~kisiel/prospe.htm>.

[25] J. Kraitchman, *Am. J. Phys.* **1953**, *21*, 17–24.

[26] C. C. Costain, *Trans. Am. Crystallogr. Assoc.* **1966**, *2*, 157–164.

[27] M. Juanes, N. Vogt, J. Demaison, I. León, A. Lesarri, H. D. Rudolph, *Phys. Chem. Chem. Phys.* **2017**,*19*, 29162–29169

[28] R. Hakiri, N. Derbel, W. C. Bailey, H. V. L. Nguyen, H. Mouhib, *Mol. Phys.* **2020**. DOI: 10.1080/00268976.2020.1728406

[29] J. Demaison, M. K. Jahn, E. J. Cocinero, A. Lesarri, J.-U. Grabow, J.-C. Guillemin, H. D. Rudolph, *J. Phys. Chem. A* **2013**, *117*, 2278–2284.

[30] J. Demaison, A. G. Császár, L. D. Margulès, H. D. Rudolph, *J. Phys. Chem. A* **2011**, *115*, 14078–14091.

[31] B. J. Esselman, B. K. Amberger, J. D. Shutter, M. A. Daane, J. F. Stanton, R. C. Woods, R. J. McMahon, *J. Chem. Phys.* **2013**, *139*, 224304.

[32] S. Herbers, P. Kraus, J.-U. Grabow, *J. Chem. Phys.* **2019**, *150*, 144308.

[33] Z. Kisiel, *J. Mol. Spectrosc.* **2003**, *218*, 58−67.

[34] D. W. J. Cruickshank, R. A. Sparks, *Proc. R. Soc. Lond. A* **1960**, 258

[35] A. Stanger, *J. Am. Chem. Soc.* **1991**, *113*, 8277–8280

[36] L. Nygaard, J. T. Nielsen, J. Kirchheiner, G. Maltesen, J. R. Andersen, G. O. Sorensen, *J. Mol. Struct.* **1969**, *3*, 491–506.

[37] A. Kumar, J. Sheridan, O. L. Stiefvater, *Z. Naturforsch.* **1978**, *33a*, 145–152.

[38] Y. Ohshima, R. Kanya, Y. Sumiyoshi, Y. Endo, *J. Mol. Spectrosc.* **2004**, *223*, 148–151.
[39] M. K. Jahn, J.-U. Grabow, M. J. Travers, D. Wachsmuth, P. D. Godfrey, D. McNaughton, *Phys. Chem. Chem. Phys.* 2017, 19, 8970–8976.
[40] T. Oka, *J. Mol. Struct.* **1995**, *352–353*, 225–233.
[41] J.-U. Grabow, W. Stahl, H. Dreizler, *Rev. Sci. Instrum.* **1996**, *67*, 4072–4084

WILEY-VCH

Entry for the Table of Contents

FULL PAPER

The interplay of microwave rotational spectroscopy and quantum chemistry leads to highly accurate geometry parameters of coumarin. Perturbations of the π electron delocalization are reflected in the bond lengths and bond angles. The large, negative inertial defect indicates pronounced out-of-plane motions of the ring.

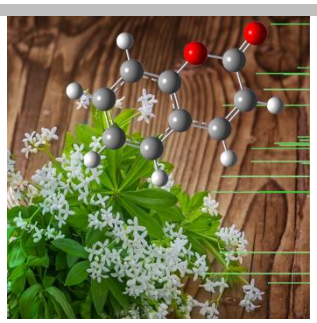

Ha Vinh Lam Nguyen, Jens-Uwe Grabow*

Page No. – Page No.

The scent of maibowle – π electron localization in coumarin from its microwave-determined structure

WILEY-VCH